Atomic force microscopy and x-ray photoelectron spectroscopy studies of ZnO nanoparticles on SiO_2 fabricated by ion implantation and thermal oxidation

H. Amekura, O. A. Plaksin, M. Yoshitake, Y. Takeda, N. Kishimoto, and Ch. Buchal

Citation: Appl. Phys. Lett. **89**, 023115 (2006); doi: 10.1063/1.2221507
View online: https://doi.org/10.1063/1.2221507
View Table of Contents: http://aip.scitation.org/toc/apl/89/2
Published by the American Institute of Physics

Atomic force microscopy and x-ray photoelectron spectroscopy studies of ZnO nanoparticles on SiO_2 fabricated by ion implantation and thermal oxidation

H. Amekura,[a] O. A. Plaksin, M. Yoshitake, Y. Takeda, and N. Kishimoto
National Institute for Materials Science, 3-13 Sakura, Tsukuba, Ibaraki 305-0003, Japan

Ch. Buchal
Institut fuer Schichten und Grenzflaechen (ISG1-IT), Forschungszentrum Juelich GmbH, D-52425 Juelich, Germany

(Received 16 March 2006; accepted 24 May 2006; published online 13 July 2006)

The morphology and chemical composition of the surface of SiO_2 that had been implanted with Zn ions of 60 keV and annealed in two different atmospheres, i.e., oxygen gas and a vacuum, were compared. In the as-implanted state, the surface mainly consisted of SiO_2 with low roughness due to radiation-induced smoothing. A large number of domelike structures of ZnO appeared on the surface of the SiO_2 after annealing in oxygen gas at 600 °C for 1 h, and the size increased with the annealing temperature up to 800 °C. After annealing at 900 °C, the surface roughness steeply decreased and the composition changed to Zn_2SiO_4. © *2006 American Institute of Physics*.
[DOI: 10.1063/1.2221507]

Zinc oxide (ZnO) has recently been receiving considerable attention because this material is a wide-gap semiconductor with a large exciton binding energy of 60 meV, which stabilizes the excitons even at room temperature.[1] Because of the concentrated oscillator strength with respect to exciton transitions, laser action is easily attainable even in nanostructures. Moreover, new lasing phenomena characteristic of nanostructures have been observed including random laser[2] and self-formed cavity laser.[3] Nanostructures of ZnO are highly attractive for light-emitting/laser applications, and various attempts have been made to fabricate ZnO nanostructures of high quality.

One of these is ion implantation combined with thermal oxidation (IICTO).[4–6] In this method, Zn metal nanoparticles (NPs) are formed in transparent insulators such as silica glass (SiO_2) by Zn-ion implantation of several tens to a few hundreds of keV. The implanted samples are then annealed in an oxidizing atmosphere so that the Zn metal NPs are oxidized to ZnO NPs. Although the annealing in oxygen gas at 700 °C for 1 h oxidizes all the Zn NPs to ZnO phase,[5] the annealing at 600 °C for 1 h oxidizes only limited portion of the Zn NPs. However, the sample annealed at 600 °C shows a strong exciton photoluminescence (PL) peak without broad defect bands, while the sample annealed at 700 °C shows relatively strong defect band.[6] Understanding of the mechanism of the *defect-band-free* PL is important also for applications.

On the other hand, Liu *et al.*[4] have assumed from the results of x-ray photoelectron spectroscopy (XPS) that the ZnO NPs were formed on the surface of the SiO_2 substrate, not embedded in the SiO_2. This provides a striking contrast to the NiO and CuO nanophases fabricated by the IICTO method, which always form NPs embedded in the SiO_2 substrate.[7–9] Because Zn ions are implanted to a region of 10–70 nm depth in the SiO_2 substrate, and because ZnO nanostructures are formed on the surface of the SiO_2 substrate, significant transportation of Zn element from the inside of the SiO_2 substrate toward the surface is expected during thermal oxidation.

In this letter, we describe a study in which the evolution of the surface morphology was monitored by atomic force microscopy (AFM) and XPS to detect the consequences of the significant transportation of Zn element from the inside of the SiO_2 substrate and the formation of ZnO nanostructures on the SiO_2 surface. This study aimed to understand the fundamental processes of ZnO NP formation by IITCO method, and to collect basic knowledge to understand the mechanism of the defect-band-free PL.

Since AFM is highly sensitive to the surface morphology but cannot detect the chemical composition of the surface structures, XPS is a good counterpart, which is highly sensitive to the surface composition but cannot detect the surface morphology. However, the chemical shift in XPS between the Zn and ZnO states is still controversial,[10] although it has been confirmed that metallic Zn shows the $2p_{3/2}$ XPS line at 1021.8 eV in the binding energy. Value of the chemical shift[4,10,11] of ZnO ranging between 0 and 0.7 eV, i.e., even including "vanishing" shift, have been reported in the literature. At present, we believe that XPS is not reliable for distinguishing ZnO from Zn. It should be noted that some past reports[4,11] have identified the formation of the ZnO phase from the chemical shift of the Zn $2p_{3/2}$ XPS line. We suspect that what was observed in these studies was a chemical shift due to the formation of an unintended Zn_2SiO_4 phase, which shows the $2p_{3/2}$ XPS line at 1023.0 eV with a large chemical shift.[12] In the present study, we have applied not only XPS but also a more reliable method, x-ray excited Auger electron spectroscopy (XAES), to distinguish the chemical shifts of Zn-related phases.

Optical-grade silica glasses of the KU-1 type (OH^-, 820 ppm), 15 mm in diameter and 0.5 mm in thickness, were implanted with $^{64}Zn^+$ ions of 60 keV up to a fluence of 1.0×10^{17} ions/cm^2. The ion flux was limited to less than 2 μA/cm^2 in order to maintain the sample temperature at

[a]Author to whom correspondence should be addressed; electronic mail: amekura.hiroshi@nims.go.jp

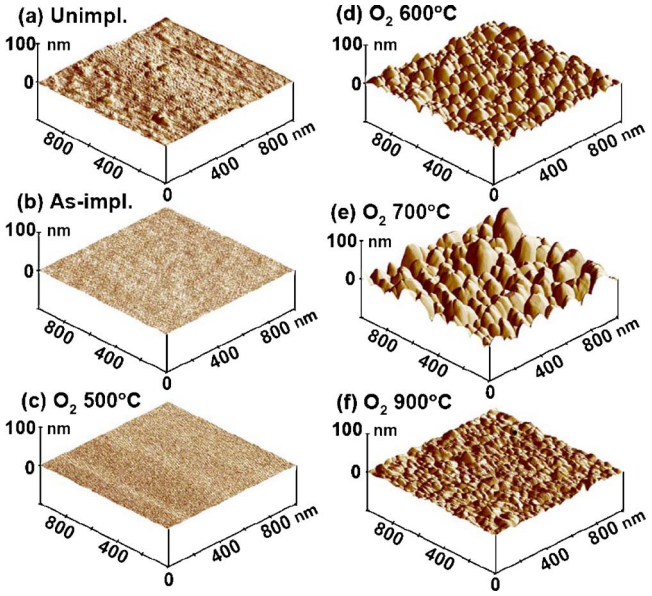

FIG. 1. (Color online) Evolution of the surface morphology of SiO_2 samples induced by Zn-ion implantation of 60 keV to a fluence of 1.0×10^{17} ions/cm^2 and subsequent annealing in oxygen gas of ~760 torr detected by AFM, before implantation (a), in the as-implanted state (b), and after annealing for 1 h at 500 °C (c), 600 °C (d), 700 °C (e), and 900 °C (f).

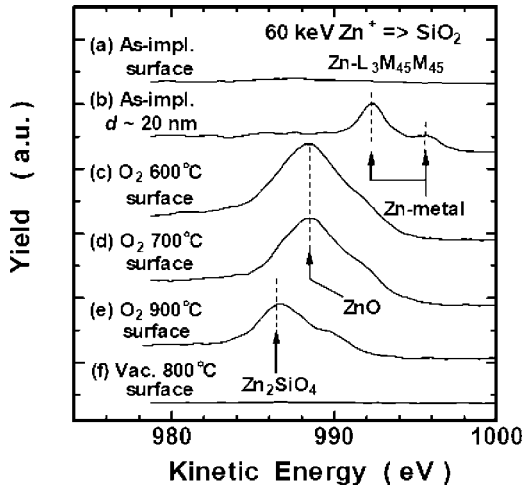

FIG. 2. XAES spectra around Zn-$L_3M_{45}M_{45}$ transitions from SiO_2 samples implanted with Zn ions of 60 keV to a fluence of 1.0×10^{17} ions/cm^2 and subsequent annealing for 1 h, in the as-implanted state (a) and (b), and after annealing for 1 h at 600 °C in O_2 gas (c), 700 °C in O_2 (d), 900 °C in O_2, (e) and 800 °C in a vacuum (f). All of the spectra were detected at the surface without sputtering except (b), which was detected after sputtering out of the surface layer of ~20 nm thick.

below 100 °C during implantation. The projected ranges of 46 and 27 nm were calculated for Zn ions of 60 keV in SiO_2 by the SRIM2003 (Ref. 13) and TRIDYN codes,[14] respectively. The TRIDYN code includes sputtering loss, whereas the SRIM code does not. The implanted samples were annealed for 1 h in a tube furnace at a temperature between 400 and 900 °C under flowing oxygen gas of ~100 SCCM (SCCM denotes cubic centimeter per minute at STP) at a pressure of $\sim1.0\times10^5$ Pa. For comparison, another set of implanted samples was annealed under the same conditions except in an annealing atmosphere consisting of a vacuum of less than 1×10^{-3} Pa instead of oxygen gas.

The surface morphology was observed by AFM in the tapping mode with a scanning area of 1×1 μm^2. XPS and XAES were carried out using a monochromatized Al $K\alpha$ x-ray source ($h\nu$=1486.7 eV) with an electron neutralizer and a hemispherical electron analyzer with a detection angle of 45°. Judging from the stability of the observed energies of the Zn $2p_{3/2}$, Zn-LMM, Si $2p$, and O $1s$ lines, and comparisons with the values reported in the literature, the samples were determined to be mostly free of significant charging due to the electron neutralizer. The atomic concentration was estimated from the peak areas of the Zn-LMM, Si $2p$, O $1s$, and C $1s$ lines using relative sensitivity factors of 2.911, 0.368, 0.733, and 0.314, respectively. Although most of the XAES and XPS spectra were taken from the surface without sputtering, some spectra were also taken after sputtering using an Ar^+ ion beam of 1 kV and 25 nA with an incident angle of 45°.

Figure 1 shows the evolution of the surface morphology of a SiO_2 sample induced by implantation of Zn ions and sequential annealing in oxygen gas. As shown in Fig. 1(a), surface roughness (R_q), i.e., the root mean square of height deviation, with a value of 1.51 nm was observed before the implantation, which was probably due to the industrial polishing processes used. After the implantation, R_q decreased to 0.39 nm, as shown in Fig. 1(b); that is, a form of radiation-induced surface smoothing[15,16] was induced. We have also carried out the step-height measurements at boundaries between implanted and unimplanted regions of the as-implanted samples at the fluences of 2×10^{16}, 5×10^{16}, and 1×10^{17} ions/cm^2. The values of the step heights were almost consistent with the calculated values of TRIDYN code,[14] i.e., the sputtering loss is not unusual.

Curve (a) in Fig. 2 shows the XAES spectrum around the Zn-$L_3M_{45}M_{45}$ edge from the surface of the Zn-implanted SiO_2 in the as-implanted state. Almost no Zn-related signal is observed. It was confirmed from the XPS spectrum (not shown) that the surface mostly consisted of Si and O atoms, apart from a low concentration of Zn atoms and residual carbon contamination. This is reasonable because the incident Zn ions have a very high energy of 60 keV, and do not stop on the surface nor in a region shallower than ~10 nm. As shown in curve (b) in Fig. 2, a twin-peak structure from the Zn metallic state is observed at 992.2 and 995.6 eV in the kinetic energy after sputtering removal of ~20 nm depth, indicating formation of the Zn metallic phase inside.

As shown in Fig. 1(c), the surface is as smooth as in the as-implanted state when R_q is maintained at less than ~0.4 nm with annealing at up to 500 °C for 1 h in oxygen gas. After 600 °C annealing [Fig. 1(d)], numerous domelike structures appear. As the annealing temperature increases from 600 to 800 °C, the size of the domelike structures increases. The corresponding value of R_q increases to 6.92, 13.0, and 16.5 nm at 600, 700, and 800 °C, respectively. The annealing temperature dependence of R_q is summarized in Fig. 3. As shown in curves (c) and (d) in Fig. 2, the domelike structures consist of ZnO, which exhibits a broad XAES peak at around 988.1 eV. The distinct migration of Zn atoms toward the surface side is also confirmed by Rutherford backscattering spectrometry (RBS).[17]

After 900 °C annealing for 1 h in oxygen gas, R_q steeply decreases to 2.89 nm. As shown in Fig. 1(f), the surface structure no longer has domelike shapes but what could be described as winding patterns. This is due to the transfor-

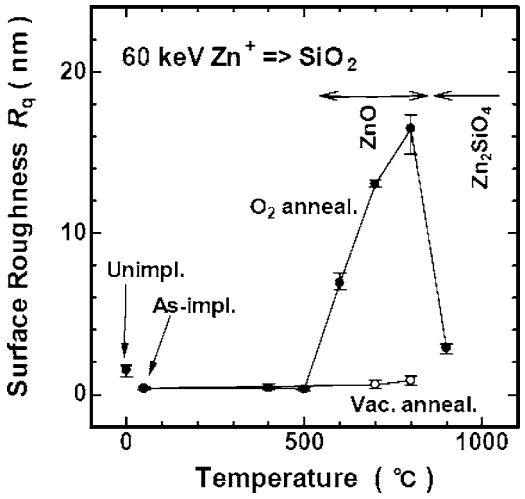

FIG. 3. Annealing temperature dependence of the surface roughness R_q of SiO_2 samples implanted with Zn ions of 60 keV to a fluence of 1.0×10^{17} ions/cm^2 and subsequent annealing for 1 h, in oxygen gas of ~760 torr (closed circles) and in a vacuum of less than 1×10^{-5} torr (open circles). The values before implantation and in the as-implanted state are also shown.

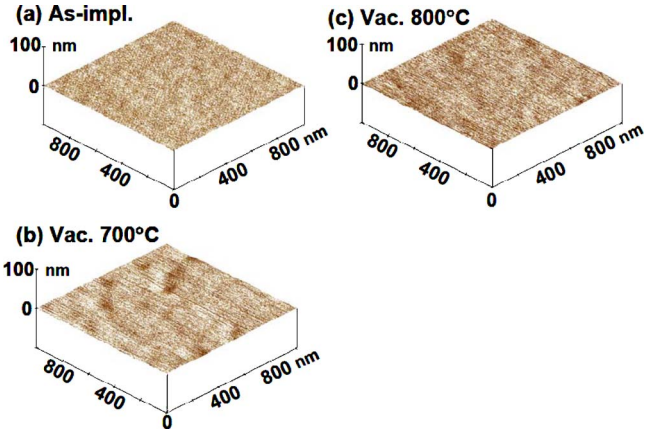

FIG. 4. (Color online) Evolution of the surface morphology of SiO_2 samples induced by Zn-ion implantation of 60 keV to a fluence of 1.0×10^{17} ions/cm^2 and subsequent annealing in a vacuum of less than 1×10^{-5} torr detected by AFM, in the as-implanted state (a) and after annealing for 1 h at 700 °C (b) and 800 °C (c).

mation of the surface composition from ZnO to Zn_2SiO_4, which is supported by a peak shift to 986.1 eV in XAES spectrum (e) of Fig. 2. Cross-sectional transmission electron microscopy (TEM) observation[6] indicated that the Zn_2SiO_4 phase has a layerlike structure covering most of the surface, whereas the ZnO phase prefers particlelike shapes covering the surface as domelike structures. The higher affinity of the Zn_2SiO_4 phase than the ZnO phase to the SiO_2 substrate is probably due to the fact that the Zn_2SiO_4 phase is formed by a reaction between the ZnO phase and the SiO_2 substrate. The Zn_2SiO_4 phase probably accommodates itself to the SiO_2 substrate by forming transition layers of nonstoichiometric Zn-deficient Zn_2SiO_4 between the stoichiometric Zn_2SiO_4 phase and the SiO_2 substrate.

The surface morphology was studied with annealing under the same conditions except for the use of a vacuum as the annealing atmosphere instead of oxygen gas. The results are shown in Fig. 4. Although R_q slightly increases from the as-implanted value of 0.39 nm to 0.62 and 0.88 nm after vacuum annealing at 700 and 800 °C, respectively, the surface always has a very smooth appearance even after vacuum annealing at up to 800 °C. No significant presence of Zn-related signals was observed on the surface by XAES after annealing at up to 800 °C for 1 h in a vacuum. RBS results showed that the drastic migration of Zn atoms toward the surface side, which was clearly observed under oxidizing annealing, was not observed after vacuum annealing.[17] Zn-related structures on the SiO_2 substrates are not formed by annealing in vacuum, but in an oxidizing atmosphere.[18]

The drastic differences in surface morphology induced by the different annealing atmospheres, namely, oxygen gas (at $\sim 1 \times 10^5$ Pa) and a vacuum (at $< 1 \times 10^{-3}$ Pa), are explained by the high vapor pressure of Zn metal. At temperature $T \sim 210$ °C or higher, the vapor pressure of Zn metal overcomes the annealing pressure of 10^{-5} torr during vacuum annealing.[18] Once the Zn atoms reach the surface by thermally activated diffusion during vacuum annealing ($\sim 1 \times 10^5$ Pa) at higher than ~210 °C, they are all effused to the atmosphere. On the other hand, under annealing in oxygen gas, Zn atoms that have reached the surface react with oxygen, and form ZnO NPs on the surface at lower than 900 °C. ZnO is more stable than metallic Zn at elevated temperatures.

[1] U. Ozgur, Ya. I. Alivov, C. Liu, A. Teke, M. A. Reshchikov, S. Dogan, V. Avrution, S.-J. Cho, and H. Morkoc, J. Appl. Phys. **98**, 041301 (2005).
[2] H. Cao, Y. G. Zhao, S. T. Ho, E. W. Seelig, Q. H. Wang, and R. P. H. Chang, Phys. Rev. Lett. **82**, 2278 (1999).
[3] M. Kawasaki, A. Ohtomo, I. Ohkubo, H. Koinuma, Z. K. Tang, P. Yu, G. K. L. Wong, B. P. Zhang, and Y. Segawa, Mater. Sci. Eng., B **56**, 239 (1998).
[4] Y. X. Liu, Y. C. Liu, D. Z. Shen, G. Z. Zhong, X. W. Fan, X. G. Kong, R. Mu, and D. O. Henderson, J. Cryst. Growth **240**, 152 (2002).
[5] H. Amekura, N. Umeda, Y. Sakuma, N. Kishimoto, and Ch. Buchal, Appl. Phys. Lett. **87**, 013109 (2005).
[6] H. Amekura, N. Umeda, Y. Sakuma, O. A. Plaksin, Y. Takeda, N. Kishimoto, and Ch. Buchal, Appl. Phys. Lett. **88**, 153119 (2006).
[7] H. Amekura, N. Umeda, Y. Takeda, J. Lu, and N. Kishimoto, Appl. Phys. Lett. **85**, 1015 (2004).
[8] H. Amekura, N. Umeda, Y. Takeda, J. Lu, K. Kono, and N. Kishimoto, Nucl. Instrum. Methods Phys. Res. B **230**, 193 (2005).
[9] H. Amekura, K. Kono, Y. Takeda, and N. Kishimoto, Appl. Phys. Lett. **87**, 153105 (2005).
[10] J. F. Moulder, W. F. Stickle, P. E. Sobol, and K. D. Bomben, *Handbook of X-ray Photoelectron Spectroscopy* (Physical Electronics, Eden Prairie, 1995).
[11] J. K. Lee, C. R. Tewell, R. K. Schulze, M. Nastasi, D. W. Hamby, D. A. Lucca, H. S. Jung, and K. S. Hong, Appl. Phys. Lett. **86**, 183111 (2005).
[12] H. Amekura (unpublished).
[13] J. F. Ziegler, J. P. Biersack, and U. Littmark, *The Stopping and Range of Ions in Solids* (Pergamon, New York, 1985), Chap. 5.
[14] W. Moeller and W. Eckstein, Nucl. Instrum. Methods Phys. Res. B **9**, 814 (1984).
[15] P. D. Townsend, P. J. Chandler, and L. Zhu, *Optical Effects of Ion Implantation* (Cambridge University Press, Cambridge, 1994), Chap. 1.
[16] K. Oyoshi, T. Tagami, and S. Tanaka, Jpn. J. Appl. Phys., Part 1 **30**, 1854 (1991).
[17] H. Amekura, N. Umeda, M. Yoshitake, K. Kono, N. Kishimoto, and Ch. Buchal, J. Cryst. Growth **287**, 2 (2006).
[18] *Tables of Physical Constants*, New ed. (Asakura, Tokyo, 1978) (in Japanese).